



HAL
open science

The CymR Regulator in Complex with the Enzyme CysK Controls Cysteine Metabolism in *Bacillus subtilis*

Catherine Tanous, Olga Soutourina, Bertrand Raynal, Marie-Françoise Hullo, Peggy Mervelet, Anne-Marie Gilles, Philippe Noirot, Antoine Danchin, Patrick England, Isabelle Martin-Verstraete

► To cite this version:

Catherine Tanous, Olga Soutourina, Bertrand Raynal, Marie-Françoise Hullo, Peggy Mervelet, et al.. The CymR Regulator in Complex with the Enzyme CysK Controls Cysteine Metabolism in *Bacillus subtilis*. *Journal of Biological Chemistry*, 2008, 283 (51), pp.35551 - 35560. 10.1074/jbc.m805951200 . pasteur-03525653

HAL Id: pasteur-03525653

<https://pasteur.hal.science/pasteur-03525653>

Submitted on 14 Jan 2022

HAL is a multi-disciplinary open access archive for the deposit and dissemination of scientific research documents, whether they are published or not. The documents may come from teaching and research institutions in France or abroad, or from public or private research centers.

L'archive ouverte pluridisciplinaire **HAL**, est destinée au dépôt et à la diffusion de documents scientifiques de niveau recherche, publiés ou non, émanant des établissements d'enseignement et de recherche français ou étrangers, des laboratoires publics ou privés.



Distributed under a Creative Commons Attribution 4.0 International License

The CymR Regulator in Complex with the Enzyme CysK Controls Cysteine Metabolism in *Bacillus subtilis**

Received for publication, August 1, 2008, and in revised form, October 15, 2008. Published, JBC Papers in Press, October 29, 2008, DOI 10.1074/jbc.M805951200

Catherine Tanous^{‡¶¶}, Olga Soutourina^{‡¶1}, Bertrand Raynal^{§||}, Marie-Françoise Hullo^{‡¶}, Peggy Mervelet^{**}, Anne-Marie Gilles^{‡¶}, Philippe Noirots^{**}, Antoine Danchin^{‡¶}, Patrick England^{§||2}, and Isabelle Martin-Verstraete^{‡¶3}

From the Institut Pasteur, [‡]Unité de Génétique des Génomes Bactériens, [§]Plate-forme de Biophysique des Macromolécules et de leurs Interactions, [¶]CNRS, URA2171, and ^{||}CNRS, URA2185, 25 rue du Docteur Roux, 75724 Paris cedex 15, France, and INRA ^{**}Mathématique, Informatique et Génome and ^{**}Unité de Génétique Microbienne, F-78352, Jouy-en-Josas, France

Several enzymes have evolved as sensors in signal transduction pathways to control gene expression, thereby allowing bacteria to adapt efficiently to environmental changes. We recently identified the master regulator of cysteine metabolism in *Bacillus subtilis*, CymR, which belongs to the poorly characterized Rrf2 family of regulators. We now report that the signal transduction mechanism controlling CymR activity in response to cysteine availability involves the formation of a stable complex with CysK, a key enzyme for cysteine biosynthesis. We carried out a comprehensive quantitative characterization of this regulator-enzyme interaction by surface plasmon resonance and analytical ultracentrifugation. We also showed that *O*-acetylserine plays a dual role as a substrate of CysK and as an effector modulating the CymR-CysK complex formation. The ability of *B. subtilis* CysK to bind to CymR appears to be correlated to the loss of its capacity to form a cysteine synthase complex with CysE. We propose an original model, supported by the determination of the intracellular concentrations of the different partners, by which CysK positively regulates CymR in sensing the bacterial cysteine pool.

Bacteria have been particularly inventive to survive in a diversity of environments by developing mechanisms of regulation of gene expression as complex as those found in eukaryotic cells (1). They efficiently adapt to environmental changes by linking gene expression to intracellular pools of key metabolites in various ways. In most cases, these effector molecules act either by directly binding to transcriptional regulators or via specific receptors as observed for two-component regulatory systems and sigma-antisigma factors. However, in the cell, the enzymes are the most suitable to inform about metabolite avail-

ability. They specifically recognize their substrates or allosteric effectors and often undergo conformational changes upon binding or during enzymatic reaction. Several enzymes have evolved as sensors in signal transduction pathways controlling gene expression. These bifunctional proteins, which are active as well in metabolism as in regulation, are called trigger enzymes (2). Some enzymes can directly bind to DNA (BirA, PutA, NadR, and PepA) or RNA (CitB), whereas phosphotransferase system components control the activity of transcription factors by phosphorylation events. However, the most abundant class of trigger enzymes modulates the transcriptional activity of regulators by protein-protein interactions. For instance, enzymes MalK, Aes, and MalY form complexes with the MalT activator (3, 4). These enzymes antagonize the binding of maltotriose, the co-activator of MalT. In the control of nitrogen metabolism in *Bacillus subtilis*, glutamate dehydrogenase (RocG) and glutamine synthetase are able to interact, respectively, with the GltC activator or the TnrA repressor and to inactivate them concomitantly (5, 6). Here, we report that CysK, the *O*-acetylserine thiol-lyase of *B. subtilis*, has acquired a regulatory function and is therefore a trigger enzyme acting as a repressor in the regulation of cysteine metabolism by an original mechanism.

In bacteria, some archaea and plants, cysteine biosynthesis proceeds via a two-step pathway involving CysK and CysE, the serine acetyl-transferase. CysE catalyzes the acetylation of L-serine by acetyl-CoA to give *O*-acetyl-L-serine (OAS)⁴. The OAS-thiol-lyase, CysK, then converts OAS and sulfide into L-cysteine and acetate. According to its catalytic mechanism, CysK belongs to the fold type II group of pyridoxal 5'-phosphate (PLP)-dependent enzymes (7). In *Salmonella typhimurium*, *Escherichia coli*, *Haemophilus influenzae*, *Mycobacterium tuberculosis*, and higher plants, CysE and CysK form a hienzyme complex, called cysteine synthase (8–10). The function of the complex is not metabolic channeling but rather a modulation of the activity of each enzyme in the complex. This association of serine acetyl-transferase and OAS-thiol-lyase provides a regulatory mechanism for cysteine biosynthesis in plants (11).

In line with the crucial role of cysteine in cellular physiology and with the reactivity of its SH group, the transport, the bio-

* This work was supported by Centre National de la Recherche Scientifique Grant URA 2171, Agence Nationale de la Recherche Grant NT05-2-44860, and Institut Pasteur Grant PTR256. The costs of publication of this article were defrayed in part by the payment of page charges. This article must therefore be hereby marked "advertisement" in accordance with 18 U.S.C. Section 1734 solely to indicate this fact.

¹ Assistant professor at the "Université Paris 7."

² To whom correspondence may be addressed: Plateforme de Biophysique des Macromolécules et de leurs Interactions, Institut Pasteur, France. Tel.: 33-1-44-38-94-74; Fax: 33-1-44-38-94-71; E-mail: patrick.england@pasteur.fr.

³ Associate professor at the "Université Paris 7." To whom correspondence may be addressed: Unité de Génétique des Génomes Bactériens, URA CNRS 2171, Institut Pasteur, France. Tel.: 33-1-40-61-35-61; Fax: 33-1-45-68-89-48; E-mail: isabelle.martin-verstraete@pasteur.fr.

⁴ The abbreviations used are: OAS, *O*-acetyl-L-serine; PLP, pyridoxal 5'-phosphate; MBP, maltose-binding protein; Ni-NTA, nickel-nitrilotriacetic acid; RU, resonance units; SPR, surface plasmon resonance; BD, DNA-binding domain; AD, activation domain; HPLC, high pressure liquid chromatography; HTH, helix turn helix.

CymR-CysK Regulatory Complex

TABLE 1

Strains and plasmids used in this study

spc is a spectinomycin resistance gene. Ap^R indicates ampicillin resistance; Km^R indicates kanamycin resistance; and Cm^R indicates chloramphenicol resistance.

Genotypes and characteristics		Source or reference
Strains		
<i>B. subtilis</i>		
168	<i>trpC2</i>	Laboratory stock
BSIP1304	<i>trpC2 ΔcysK::spc</i>	Ref. 56
BSIP1798	<i>trpC2 ΔcymR amyE::aphA3 lacZ</i>	Ref. 20
<i>E. coli</i>		
DH5α	F' Phi80 <i>dlacZ</i> ΔM15 Δ(<i>lacZYA-argF</i>)U169 <i>deoR recA1 endA1 hsdR17</i> (rK-mK+) <i>phoA supE44 lambda-thi-1</i>	Commercial (Invitrogen)
BL21	F ⁻ <i>ompT hsdS_B(r_B⁻m_B⁻) gal dcm</i>	Commercial (Invitrogen)
<i>S. cerevisiae</i>		
PJ69-4 a/α	MATa/α <i>trp1-901 leu2-3,112 ura3-52 his3-200 gal4Δ gal80Δ</i> LYS2::GAL1-HIS3 GAL2-ADE2 met2::GAL7-lacZ	Ref. 22
Plasmids		
pTYB11	Expression vector, T7 promoter N-terminal Intein-CBD fusion, Ap ^R	Commercial (Biolabs)
pMAL-c2X	Expression vector, tac promoter, N-terminal MBP fusion, Ap ^R	Commercial (Biolabs)
pET22b	Expression vector, T7 promoter, C-terminal His tag fusion, Ap ^R	Commercial (Novagen)
pET28a	Expression vector, T7 promoter, N-terminal His tag fusion Km ^R	Commercial (Novagen)
pDIA17	pACYC184 carrying <i>lacI</i> ; Cm ^R	Ref. 25
pGBDU-C1	Expression vector for use in two-hybrid analysis	Ref. 22
pGAD-C1	Expression vector for use in two-hybrid analysis	Ref. 22
pDIA5575	pΔ <i>FytlI'</i> - <i>lacZ</i>	Ref. 20
pDIA5647	pGAD-C1 derivative carrying <i>cysK</i> gene	Ref. 20
pDIA5653	pGBDU-C1 derivative carrying <i>cysK</i> gene	This study
pDIA5686	pET22b derivative carrying <i>mccA</i> gene	Ref. 19
pDIA5708	pET22b derivative carrying <i>cysK</i> gene	Ref. 19
pDIA5770	pTYB11 derivative carrying <i>cymR</i> gene	Ref. 19
pDIA5778	pGBDU-C1 derivative carrying <i>cysE</i> gene	This study
pDIA5779	pGAD-C1 derivative carrying <i>cysE</i> gene	This study
pDIA5794	pET22b derivative carrying <i>cysE</i> gene	This study
pDIA5795	pET28a derivative carrying <i>cysE</i> gene	This study
pDIA5796	pMAL-c2X derivative carrying <i>cysK</i> gene	This study

synthesis and the degradation of this amino acid are tightly controlled in response to environmental changes. A large variety of molecular mechanisms participate in fine-tuning the regulation of cysteine metabolism in bacteria (12). The CymR regulator has recently been characterized as the central repressor of cysteine metabolism in *B. subtilis* (13). CymR belongs to the large and widespread Rrf2 family of transcription factors, which comprises the iron-sulfur cluster biogenesis regulator IscR in *E. coli* (14, 15), and the global iron-responsive regulator RirA in *Rhizobiaceae* (16). CymR controls the expression of genes involved either in cysteine synthesis from sulfide (*cysK*), sulfonates (*ssu*), or methionine (*mccAB*) or in cystine uptake (*tcyP*), by directly binding a 27-bp conserved motif in their promoter regions (13, 17). Interestingly, a large set of genes is controlled by both CymR and CysK in *B. subtilis* (13, 18). Previous experiments suggested that CysK and CymR are required to induce a DNA electrophoretic mobility shift (19). Physiological data and gel shift experiments also show that OAS, the direct precursor of cysteine, is important in the signaling pathway controlling CymR-dependent repression in the presence of cysteine (19–21).

We show in this work that CysK of *B. subtilis* interacts with CymR *in vivo* and *in vitro*. This enzyme acts as a sensor of cysteine availability in the signal transduction pathway modulating CymR activity.

EXPERIMENTAL PROCEDURES

Bacterial Strains and Plasmids—The bacterial strains and plasmids used are listed in Table 1. *E. coli* was grown in LB and *B. subtilis* in minimal medium (20) supplemented with 1 mM L-methionine or 0.5 mM L-cystine. When required, antibiotics were

added: ampicillin and spectinomycin, 100 μg/ml; chloramphenicol and kanamycin, 5 μg/ml (*B. subtilis*) or 20 μg/ml (*E. coli*).

Yeast Two-hybrid Assay—The genes *cysK* and *cysE* were fused to the genes coding for the GAL4 DNA-binding (GAL4BD) or GAL4 activation (GAL4AD) domains in vectors pGBDU-C1 (bait) or pGAD-C1 (prey) (22), resulting in plasmids pDIA5653, pDIA5647, pDIA5778, and pDIA5779 (Table 1). *Saccharomyces cerevisiae* strains PJ69-4a and PJ69-4α (22) were then transformed respectively by the bait- and prey-derived vectors. Because we failed to clone *cymR* into the pGAD and pGBDU vectors in *E. coli*, we used gap repair recombination in *S. cerevisiae* (23) to directly construct the plasmids containing the translational fusion of *cymR* with Gal4BD or Gal4AD.

The two-hybrid assays were then performed as previously described (24). Positive protein-protein interaction between the bait and a prey was detected by the ability of the cells to grow on plates with synthetic complete medium depleted for leucine, uracil, and histidine (SC-LUH) and for leucine, uracil, and adenine (SC-LUA). Interaction phenotypes were scored after 4 and 22 days of growth at 30 °C.

Overexpression and Purification of CysE, CysK, MccA, and CymR—To obtain CysE fused to a His tag at the N terminus (His₆-CysE) or at the C terminus (CysE-His₆), the *cysE* gene (+1 to +626) was amplified by PCR using primers introducing a 5'-NdeI site and a 3'-XhoI site. This fragment was cloned into pET28a or pET22b (Novagen) to form a translational fusion of *cysE* with six histidine codons at the 5' (pDIA5795) or 3' (pDIA5794) ends, respectively (Table 1). To obtain CysK fused to a maltose-binding protein (MBP) at the N terminus (MBP-CysK), the *cysK* gene (+1 to +924) was amplified by PCR using

primers introducing a 5'-XbaI site or a 3'-PstI site, and the corresponding fragment was cloned into pMAL-c2X (BioLabs), giving pDIA5796. These plasmids were introduced into *E. coli* BL21 strain (Novagen), which contains pDIA17 (25). The resulting strains were grown at room temperature in LB medium to an A_{600} of 1. Isopropyl β -D-thiogalactopyranoside (1 mM) was then added, followed by incubations for 7 h at 20 °C and 3 h at 37 °C. The cells were centrifuged and resuspended in 50 mM sodium phosphate buffer (pH 8) containing 300 mM NaCl and protease inhibitor (Complete EDTA-free; Roche Applied Science) and lysed by sonication. *E. coli* crude extracts containing His-tagged CysE were loaded on a Ni-NTA-agarose column and eluted with 300 mM imidazole. The crude extract containing MBP-CysK was loaded on an amylose column (BioLabs) and eluted with 10 mM maltose. MBP-CysK was then cleaved by the Factor X. The Factor X was removed using the Factor Xa cleavage capture kit (Novagen), whereas MBP was retained by flowing the reaction mixture through an amylose column.

CysK-His₆, MccA-His₆, and native CymR were purified as previously described (19). CymR, CysK-His₆, and MBP-CysK were subjected to a second step of purification by size exclusion chromatography on an Ultrogel AcA54 resin. The protein concentration was determined by measuring the absorbance at 280 nm using an extinction coefficient calculated from the amino acid composition of each protein.

Gel Mobility Shift Assays—The *ytll* promoter region (−86 to +22) was amplified using primers OS62 (5'-TGATTAGTCAAAGATCAGAGTATGC-3') and OS63 (5'-ATCATCACTCATTTTTGTCACCTCCTC-3'), and pDIA5575 as template (20). The PCR product was labeled using [γ -³²P]ATP 5'-end-labeled primer OS63. Unincorporated oligonucleotides were removed using the QIAquick PCR purification kit (Qiagen). Protein-DNA complexes were formed as previously described (19) and analyzed on 20% acrylamide gels. When specified, OAS (Sigma) was added to the reaction mixture at various concentrations.

In Vitro Pulldown Assays—His-tagged proteins were immobilized on the Ni-NTA-agarose resin (Qiagen). 50 μ l of Ni-NTA-agarose resin (50% (v/v) slurry) were incubated for 1 h with or without 60 μ g of CysK-His₆, MccA-His₆, or His₆-CysE in a binding buffer 50 mM sodium phosphate, pH 8.0, containing 300 mM NaCl, and 0.1% (w/v) of bovine serum albumin. The mixtures were then incubated in the presence or absence of 30 μ g of purified CymR or CysK (obtained after cleavage of MBP). After washing, the bound proteins were eluted with 250 mM imidazole.

Surface Plasmon Resonance Binding Assays—The assays were performed at 25 °C in 20 mM sodium phosphate, pH 7.0, containing 200 mM NaCl and 0.1 mM PLP. To monitor protein-protein interactions, monoclonal antibodies PentaHis (Qiagen) or anti-MBP mAb565 (26) were covalently coupled to a CM5 sensorchip, using a Biacore 2000 instrument and the Amine Coupling Kit (Biacore). Immobilization densities of \sim 10,000 resonance units (RU; 1 RU = 1 pg \cdot mm^{−2}) were achieved. His₆-CysE, CysE-His₆, MccA-His₆, MBP-CysK, or CysK-His₆ were respectively captured at densities of 150, 1800, 2000, and 1500 RU. CymR (0.1–10.5 μ M) was injected over immobilized CysK-

His₆ or MBP-CysK at a flow rate of 50 μ l \cdot min^{−1}. For the OAS dissociation experiments, 800 or 250 RU of CymR were captured on immobilized CysK-His₆ or MBP-CysK, respectively, followed by a 3-min injection of various concentrations of OAS or *N*-acetyl-serine from 0.05 to 1 mM.

A 109-bp *ytll* biotinylated promoter region was immobilized to the dextran-streptavidin matrix of a SA sensorchip, at a density of 340 RU. 1.75 μ M of either CymR or CysK-His₆, an equimolar CymR/CysK-His₆ mixture or 18 μ M of His₆-CysE, were then injected at a flow rate of 5 μ l \cdot min^{−1}. A streptavidin surface devoid of DNA was used as reference. Each assay was repeated with three independent preparations of each protein.

The association and dissociation profiles were double-referenced using the Scrubber 2.0 software (BioLogic Software), *i.e.* both the signals from the reference surfaces and from blank experiments using running buffer instead of protein were subtracted. The steady-state surface plasmon resonance (SPR) responses (R_{eq}) were plotted against the CymR concentration (C) and fitted according to a model corresponding to two binding events to independent sites,

$$R_{eq} = (R_{max1} \times C)/(K_{d1} + C) + (R_{max2} \times C)/(K_{d2} + C) \quad (\text{Eq. 1})$$

where K_{d1} and K_{d2} are the equilibrium dissociation constants of the two successive binding events, and R_{max1} and R_{max2} are the corresponding maximal binding capacities. The CymR-CysK dissociation profiles were analyzed using the following double-exponential function of time,

$$R = R_1 \times e^{-k_{off1} \times t} + (R_0 - R_1) \times e^{-k_{off2} \times t} \quad (\text{Eq. 2})$$

where R_0 is the experimental SPR signal at the start of dissociation, and R_1 is the fitted amplitude of the first dissociation phase.

The association profiles were finally fitted with an equation describing a sequential CymR association process,

$$R = (k_{on1} \times C \times R_{max1}/(k_{on1} \times C + k_{off1})) \times (1 - e^{-(k_{on1} \times C + k_{off1})t}) + ((k_{on2} \times C)/(k_{on2} \times C + k_{off2}))(k_{on1} \times C \times R_{max1}/(k_{on1} \times C + k_{off1})) \times (1 - e^{-(k_{on1} \times C + k_{off1})t}) \times (1 - e^{-(k_{on2} \times C + k_{off2})t}) \quad (\text{Eq. 3})$$

where k_{on1} and k_{on2} are the association rate constants of the two successive binding events, k_{off1} and k_{off2} are the dissociation rate constants (obtained from Equation 2), and R_{max1} is the maximal binding capacity corresponding to the first binding phase (obtained from Equation 1).

Analytical Ultracentrifugation—Sedimentation velocity and equilibrium experiments with CymR or CysK-His₆ (3 μ M or 16.5 μ M) and the equimolar CymR/CysK-His₆ mixture (3 or 16.5 μ M each), were performed at 25 °C in a ProteomeLab XL-I analytical ultracentrifuge (Beckman-Coulter) equipped with both UV-visible and Rayleigh interference detection systems, using an An60Ti rotor and 12 mm double-sector aluminum centerpieces. The software Sednterp 1.09 was used to estimate the partial specific volumes of CymR (0.745 ml \cdot g^{−1}), CysK-His₆ (0.744 ml \cdot g^{−1}), and their 1:1 complex (0.744 ml \cdot g^{−1}), as well as

CymR-CysK Regulatory Complex

the viscosity ($\eta = 0.903$ cP) and density ($\rho = 1.00587$ g·ml⁻¹) of the buffer used.

For sedimentation velocity experiments, 300 μ l of CymR or CysK-His₆ (3 or 16.5 μ M) were spun at 50,000 rpm, whereas the equimolar CymR/CysK-His₆ mixture (3 or 16.5 μ M each) was spun at 30,000 rpm. Absorbance (276 nm) and interference fringe displacement profiles were recorded every 2 min. Sedimentation coefficient continuous $c(S)$ distributions and dimerization equilibrium dissociation constants were determined using the software Sedfit 11.3 (27).

For sedimentation equilibrium experiments, 150 μ l of CymR (3 μ M), CysK-His₆ (3 μ M), or the equimolar CymR/CysK-His₆ mixture (3 μ M each) were spun sequentially at 10,000 rpm for 30 h, 13,000 rpm for 11 h, 17,000 rpm for 11 h, 21,000 rpm for 11 h, and 50,000 rpm for 3 h (to measure the base-line value). The data were recorded for each speed after controlling that sedimentation/diffusion equilibrium had been effectively reached. For each sample, the radial distributions for the two most appropriate speeds were globally fitted with the Ultrascan 9.5 software (28) using a model corresponding to the number of species detected in the sedimentation velocity experiments. Monte Carlo analysis was performed on each fit to estimate the error on the measured values.

Determination of CysK and CysE Activities—The OAS thiolase activity of CysK was determined as previously described (19). The serine acetyltransferase activity of CysE was assayed at 30 °C by monitoring the cleavage of the thioester bond of acetyl-CoA as previously described (29). The reaction rate was calculated using a differential extinction coefficient between acetyl-CoA and CoA of 3.2 mM·cm⁻¹. One unit of enzyme activity was defined as the amount of enzyme that catalyzed the formation of 1 μ mol CoA·min⁻¹·(mg of protein)⁻¹. All of the assays were performed in triplicate.

Estimation of Intracellular Protein and Metabolite Concentrations—The intracellular concentrations of CymR, CysK, OAS, and cysteine in *B. subtilis* were determined in strain 168 in MQ-S in the presence of methionine or cystine. Crude extracts and various amounts of purified CymR or CysK were loaded on an SDS-PAGE. Proteins were transferred to a polyvinylidene difluoride membrane, probed with polyclonal anti CymR or anti-CysK antibodies followed by an anti-HP rabbit antibody, and revealed using the ECL-Plus Kit (Amersham). The quantity of CymR or CysK contained in a given volume of the crude extract was estimated with the Quantity One software (Bio-Rad) by comparison with known amounts of purified proteins. Crude extracts of strain BSIP1798 (Δ cymR) and BSIP1304 (Δ cysK) were used as negative controls. To determine metabolite concentrations, the cells were suspended in a sulfosalicylic acid buffer (3% final concentration) and disrupted by shaking for 40 s at power 5 in a FastPrep cell disruptor (FP120; Savant Instruments, Inc., Holbrook, NY). Supernatant samples obtained after centrifugation were analyzed as described (19). Intracellular protein and metabolite concentrations were estimated assuming a cell volume of 6.7 μ l·(mg of total cell protein) (30) or a *B. subtilis* intracellular volume of 5 μ m³.

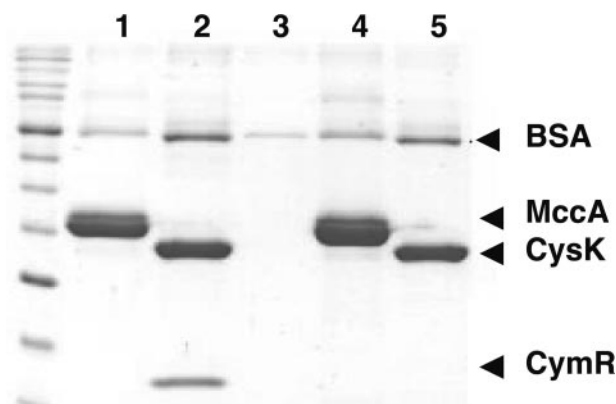


FIGURE 1. Detection of a direct interaction between CymR and CysK by His tag pull-down assay. Purified His-tagged proteins immobilized on Ni-NTA-agarose resin were incubated or not with purified CymR and eluted with imidazole. Aliquots were analyzed on a 12% SDS-PAGE gel. Lane 1, MccA-His₆ (34 kDa) incubated with purified CymR (15.4 kDa); lane 2, CysK-His₆ (34 kDa) incubated with purified CymR; lane 3, free Ni-NTA-agarose incubated with CymR; lane 4, MccA-His₆ without CymR; lane 5, CysK-His₆ without CymR.

RESULTS

CysK Interacts with CymR to Form a Complex *in Vitro*—To investigate whether CymR could interact directly and specifically with CysK in the absence of DNA, we performed pull-down assays. CysK-His₆ or MccA-His₆ (used as a control as it shares 35% identity with CysK) were bound on a Ni-NTA-agarose resin, before adding native purified CymR at a 1:1 molar ratio. CymR was co-eluted only with CysK-His₆ (Fig. 1, lane 2); no residual co-elution could be observed with MccA-His₆ or in the absence of His-tagged partner (Fig. 1, lanes 1 and 3). Thus, CymR was specifically retained on the Ni-NTA-agarose resin via its interaction with the CysK-His₆ protein. This indicated that CymR and CysK formed a stable complex *in vitro*.

To confirm the existence of a direct interaction between CysK and CymR, we performed real time SPR assays by flowing CymR, over surfaces on which CysK-His₆, MccA-His₆, or MBP-CysK had been tethered. On either the CysK-His₆ (Fig. 2A) or the MBP-CysK (data not shown) surfaces, a CymR concentration dependence of the SPR signal was observed, whereas no signal could be detected on the MccA-His₆ surface (data not shown).

Evidence for an *in Vivo* Interaction between CymR and CysK—The existence of the CymR-CysK complex was further confirmed *in vivo* by using the yeast two-hybrid system. The full-length CymR and CysK proteins were fused to either the GAL4 DNA-binding domain (BD) or the GAL4 activation domain (AD) and expressed in yeast. When CymR-AD/CysK-BD or CysK-AD/CymR-BD were co-expressed, growth of the diploid cells was observed on the selective medium (Fig. 3), indicating the existence of an interaction between CymR and CysK in *S. cerevisiae* in both setups. In contrast, we could not detect the formation of dimers of CysK or CymR by this technique. CysK from various bacteria is known to be a homodimer, but for both CysK from *Arabidopsis thaliana* and *E. coli*, no dimerization was observed in yeast two-hybrid assays (31, 32).

Determination of the Stoichiometry of the CymR-CysK Complex—The stoichiometry of the *in vitro* CymR-CysK complex was investigated by analytical ultracentrifugation using

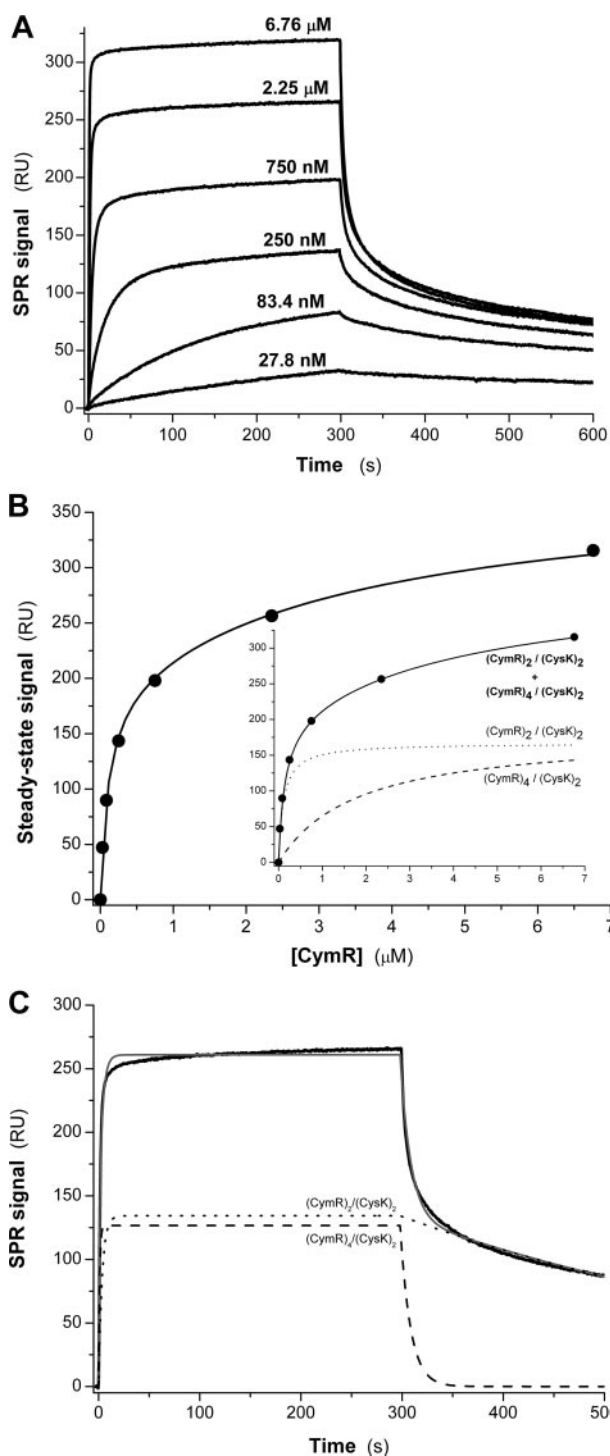


FIGURE 2. Monitoring of the binding of CymR to CysK-His₆ by surface plasmon resonance. *A*, real time association and dissociation profiles corresponding to the injection of various CymR concentrations over immobilized CysK-His₆. *B*, CymR concentration dependence of steady-state SPR signals. *Inset*, deconvolution of the steady-state signal into two components, corresponding to the formation of (CymR)₂-(CysK)₂ (dotted line) and (CymR)₄-(CysK)₂ (dashed line), respectively. *C*, the decomposition of the experimental binding profile obtained for 2.25 μM of CymR, (in black), into its (CymR)₂-(CysK)₂ (dotted line) and (CymR)₄-(CysK)₂ (dashed line) components, and global fit assuming a sequential binding (in gray).

sedimentation velocity or equilibrium experiments, at various concentrations of CymR or CysK, alone or together (Fig. 4 and Table 2). The sedimentation coefficient distribution of CysK, at

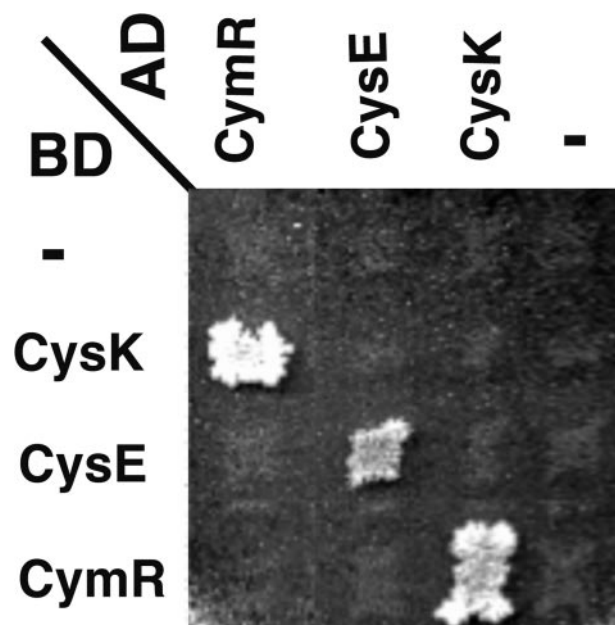


FIGURE 3. Detection of CymR/CysK interactions by yeast two-hybrid assays. Diploid yeast cells expressing the indicated combinations of proteins fused to Gal4BD (BD) and Gal4AD (AD) were selected for expression of the *His3* reporter. Binary interactions resulted in growing colonies on synthetic complete medium lacking leucine, uracil, and histidine. The Gal4AD and Gal4BD fusions are indicated on the top and left sides of the matrix, respectively. Control matings with Gal4BD and Gal4AD alone were used as negative self-activation controls.

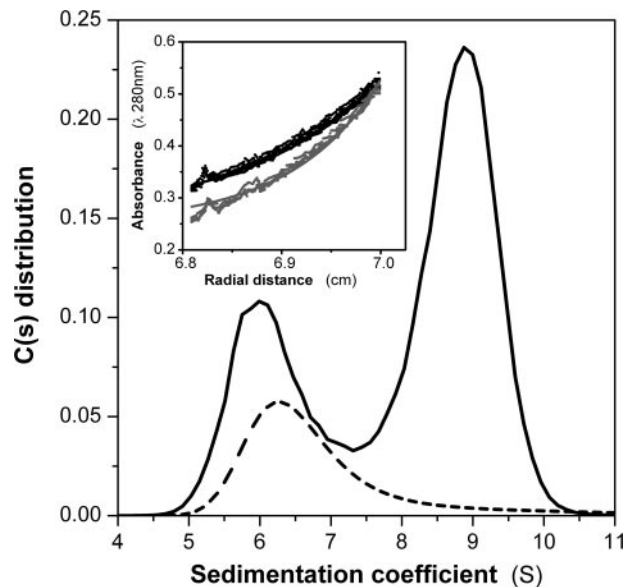


FIGURE 4. Formation of the CymR-CysK complex studied by analytical ultracentrifugation. Continuous sedimentation coefficient distribution analysis of CymR/CysK-His₆ mixtures at 3 μM (dashed line) and 16 μM (solid line). *Inset*, experimental sedimentation equilibrium radial distributions at 10,000 rpm (black) and 13,000 rpm (gray) of CymR/CysK-His₆ at 3 μM and fitted curves corresponding to a 98.5-kDa (CymR)₂-(CysK)₂ complex. Sedimentation coefficients are expressed in Svedberg: 1 S = 10⁻¹³ s.

both 3 and 16 μM, revealed the presence of a single species (4.7 S) whose molecular mass (68.0 ± 1.3 kDa) was determined by sedimentation equilibrium. This indicates that CysK is a dimer in this range of concentration, as previously observed in other bacteria (33). Similar analyses were performed for CymR. At 3 μM, they revealed one predominant species (2.2 S; 30.8 ± 2.3

TABLE 2
Sedimentation characteristics of CysK, CymR, and the CymR-CysK complex

	Concentration	$S_{w,20}$ value ^a	Percentage of total mass
	μM		%
CysK-His ₆	3	4.7 ± 0.5 S	100
	16	4.6 ± 0.2 S	100
CymR	3	2.2 ± 0.2 S	100
	16	2.4 ± 0.3 S	89
		3.8 ± 0.5 S	11
CymR/CysK-His ₆ 1:1 ratio	3	6.2 ± 0.5 S	100
	16	2.5 ± 0.2 S	16
		6.0 ± 0.5 S	27
		8.4 ± 0.6 S	57

^a All of the detected species were determined by sedimentation coefficient distribution $c(S)$ analysis of the radial distributions using the software Sedfit 11.3 (27).

kDa), corresponding to a dimer of CymR. At higher concentrations (16 μM), small quantities of another sedimenting species were detected, with an S value of 4.4 S that would be consistent with a tetrameric form of CymR. This is the first reported data concerning the oligomerization state of a member of the poorly characterized Rrf2 family of repressors. The K_d of the $(\text{CymR})_2 \leftrightarrow (\text{CymR})_4$ equilibrium could be estimated at $\sim 200 \mu\text{M}$. When CymR and CysK were mixed together at a 1:1 molar ratio, the sedimentation profiles revealed two different species whose abundance varied with the total CymR + CysK concentration. The mixture obtained with 3 μM of each protein behaved as a homogeneous species with a sedimentation coefficient of 6.2 S and a molecular mass of 98.4 ± 5.6 kDa, corresponding to a complex constituted of two CymR and two CysK molecules. However, when 16 μM of each protein were mixed, we detected the same $(\text{CymR})_2$ - $(\text{CysK})_2$ complex together with a new majority species, which sediments with a standard S value of 8.6 S that would be consistent with a $(\text{CymR})_4$ - $(\text{CysK})_4$ complex. A small proportion of unliganded CymR (either excess or inactive) could also be observed at this concentration. The K_d of the $(\text{CymR})_2$ - $(\text{CysK})_2 \leftrightarrow (\text{CymR})_4$ - $(\text{CysK})_4$ equilibrium could be estimated at $\sim 4 \mu\text{M}$.

Determination of the Energetic and Kinetic Parameters of the CymR-CysK Complex—SPR experiments were performed by flowing CymR over a CysK surface. The association and dissociation curves showed a markedly concentration-dependent biphasic behavior, whether CysK was tethered by its N terminus (MBP-CysK; data not shown) or its C terminus (CysK-His₆; Fig. 2A). The analysis of the dissociation curves revealed two parallel dissociation phases, with respective dissociation rates of $1.2 (\pm 0.2) \times 10^{-3} \text{ s}^{-1}$ ($k_{\text{off}1}$) and $0.19 \pm 0.03 \text{ s}^{-1}$ ($k_{\text{off}2}$). The first slow phase ($t_{1/2} = 600$ s) reached a maximum amplitude $R_{\text{max}1}$ corresponding to a 1:1 stoichiometric ratio between CymR and CysK, consistent with the $(\text{CymR})_2$ - $(\text{CysK})_2$ complex detected by analytical ultracentrifugation at low concentrations. On the contrary, the second fast phase ($t_{1/2} = 4$ s) could only be detected for CymR concentrations higher than 250 nM, and its amplitude increased steadily reaching a maximal value $R_{\text{max}2}$, equal to $R_{\text{max}1}$, equivalent to the binding of a second $(\text{CymR})_2$ dimer. The steady-state SPR signals, when plotted against the CymR concentration (Fig. 2B), could be optimally fitted with a two-term equation corresponding to two independent binding sites, with respective dissociation equilibrium

constants of $110 \pm 19 \text{ nM}$ (K_{d1}) and $3.5 \pm 0.6 \mu\text{M}$ (K_{d2}). By plotting the amplitudes of the two above-mentioned dissociation phases against the CymR concentration, we deduced that K_{d1} corresponds to the slow dissociation phase ($k_{\text{off}1}$), and K_{d2} corresponds to the fast dissociation phase ($k_{\text{off}2}$) (Fig. 2B, inset). Finally, the association process of CymR to the CysK surface was optimally fitted, assuming it followed a sequential process, with a first $(\text{CymR})_2$ dimer binding to $(\text{CysK})_2$ with an association rate of $1.2 (\pm 0.3) \times 10^4 \text{ M}^{-1} \cdot \text{s}^{-1}$ ($k_{\text{on}1}$), followed by a second $(\text{CymR})_2$ binding to the $(\text{CymR})_2$ - $(\text{CysK})_2$ complex with an association rate of $4.3 (\pm 0.5) \times 10^4 \text{ M}^{-1} \cdot \text{s}^{-1}$ ($k_{\text{on}2}$). The decomposition of the experimental binding profile for 2.25 μM of CymR into these two components is shown in Fig. 2C. The contribution of preformed $(\text{CymR})_4$ tetramer to the binding process could be neglected, because analytical ultracentrifugation showed that this species was virtually absent in solution for 3 μM of CymR (a concentration in the range of K_{d2}). To ascertain whether the $(\text{CymR})_4$ - $(\text{CysK})_4$ complex detected in the analytical ultracentrifugation experiments at high concentration could also be formed in the SPR experimental setup in which CysK is not in solution, a CymR/CysK-His₆ mixture (2.5 μM each) was injected onto a presaturated $(\text{CymR})_2$ - $(\text{CysK})_2$ surface. We consistently observed a stoichiometric binding of preformed $(\text{CymR})_2$ - $(\text{CysK})_2$ onto the $(\text{CymR})_2$ - $(\text{CysK})_2$ surface, showing that a $(\text{CymR})_4$ - $(\text{CysK})_4$ complex could also be formed in the conditions used for the SPR experiments (data not shown).

Modulation of the CymR-CysK Interaction by OAS—OAS, the substrate of CysK, is the signaling molecule controlling the CymR-dependent regulation (13). Although it has been shown that OAS prevents the formation of a CymR-CysK-DNA ternary complex *in vitro* (19), the mechanism of action of OAS remains unknown. We investigated by SPR the role of OAS on the formation of the CymR-CysK complex. The binding of CymR to the CysK-His₆ surface was totally prevented in the presence of 100 μM OAS. This effect was highly specific, because 5 mM of *N*-acetylserine, a close derivative of OAS, had no effect on the formation of the CymR-CysK complex (Fig. 5A).

We also evaluated by SPR the effect of OAS on the preformed $(\text{CymR})_2$ - $(\text{CysK})_2$ complex by injecting a range of concentrations of OAS (6 μM to 5 mM) onto a saturated $(\text{CymR})_2$ - $(\text{CysK})_2$ surface. OAS increased the dissociation rate of CymR-CysK in a concentration-dependent manner (Fig. 5B). k_{off} was plotted against the concentration of OAS, allowing us to determine an $[\text{OAS}]_{50}$ of $211 \pm 51 \mu\text{M}$, corresponding to the concentration of OAS required to obtain half of the maximal dissociation rate. Similar results were obtained on a $(\text{CymR})_2$ - $(\text{MBP-CysK})_2$ surface (data not shown).

Binding of CymR and CysK to the *ytII* Promoter Region—Although CymR comprises a conserved winged helix-turn-helix (HTH) DNA-binding domain, as all the other repressors of the Rrf2 family, previous gel mobility shift assay results suggested that both CysK and CymR were necessary to observe the formation of a protein-DNA complex with the *yrT* promoter region, one of the direct targets of CymR (13, 19). To obtain further insights on the DNA binding properties of CymR and its dependence on CysK, we determined, both by SPR and gel shift assays, whether purified native CymR was able to interact with

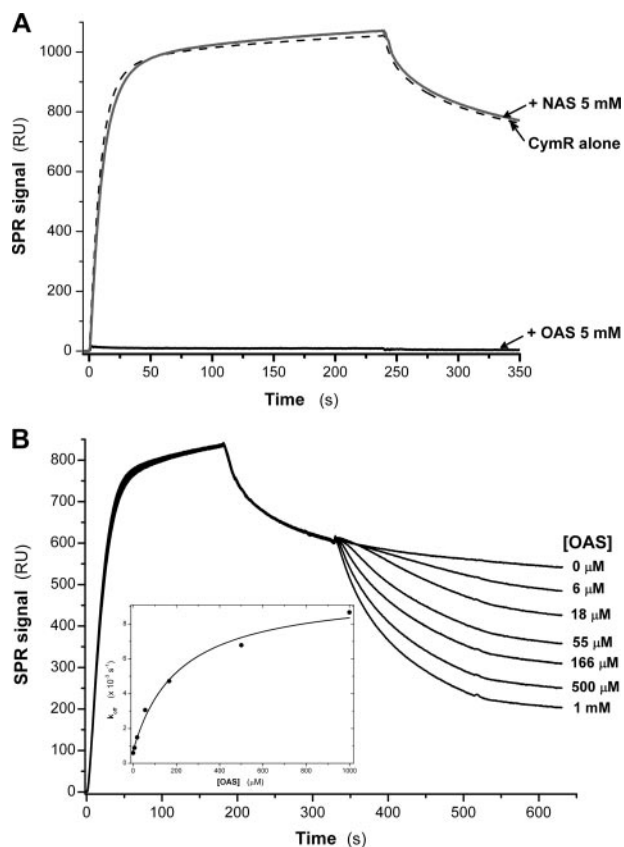


FIGURE 5. Real time SPR analysis of the effect of OAS on the CymR-CysK complex. *A*, OAS or *N*-acetyl-serine (NAS) (5 mM) were co-injected with CymR over CysK-His₆. *B*, OAS (6–1000 μ M) was injected during the dissociation of CymR from CysK-His₆. Inset: OAS concentration dependence of the dissociation rate (k_{off}) of the CymR-CysK complex.

another promoter region, *ytII*, in the presence or absence of CysK.

For the SPR experiments, a biotinylated *ytII* promoter region fragment (–86 to +22) was captured on a streptavidin surface. We observed that both CymR alone and CymR-CysK, but not CysK alone, were able to bind to the *ytII* surface (Fig. 6A). The SPR signals obtained at saturating CymR and CymR-CysK concentrations were consistent in both cases with a 4:1 stoichiometry of CymR over *ytII*. By comparing the dissociation rate of the binary *ytII*-(CymR)₄ complex with that of the ternary *ytII*-(CymR)₄-(CysK)₄ complex, we showed that the presence of CysK increased 7-fold the stability of binding of CymR to the *ytII* promoter region. Indeed, the dissociation rate in the absence of CysK was $\sim 3 \times 10^{-3} \text{ s}^{-1}$ ($t_{1/2} = 4 \text{ min}$), whereas that in the presence of CysK was $4 \times 10^{-4} \text{ s}^{-1}$ ($t_{1/2} = 30 \text{ min}$). The DNA binding ability of CymR in the absence of CysK was also shown in gel shift experiments. However, important quantities of CymR (5 μ g) were required to obtain complete *ytII* mobility retardation, which is best detected in high percentage acrylamide gels (Fig. 6B). As expected, similar quantities of CysK alone did not induce any *ytII* mobility retardation (Fig. 6B, lane 5). Interestingly, when a preformed CymR-CysK complex was incubated with the *ytII* promoter fragment, full retardation was obtained for protein amounts as low as 250 ng of CymR, mixed with 500 ng of CysK (Fig. 6B, lane 7), in agreement with our previous observation for the *yrpT* promoter region.

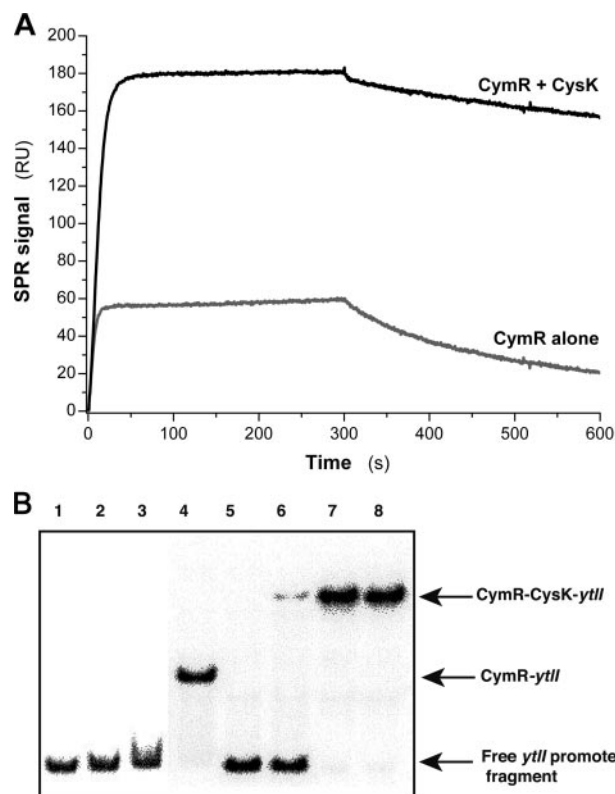


FIGURE 6. Monitoring of the interaction of CymR with DNA in the presence or absence of CysK by real time SPR (*A*) or by gel shift experiments (*B*). *A*, association and dissociation profiles corresponding to the injection of CymR (1.75 μ M) or preformed CymR-CysK complex (1.75 μ M each), over the immobilized *ytII* promoter. *B*, CymR- and CysK-dependent retardation of the *ytII* promoter region mobility. Lane 1, free *ytII*; lanes 2–4, *ytII* with increasing amounts (1, 2.5, and 5 μ g, respectively) of purified CymR; lane 5, *ytII* with 5 μ g of purified CysK; lanes 6–8, *ytII* with increasing amounts of 1:1 molar ratio CymR-CysK mixtures (50:100, 150:300, and 250:500 ng of CymR and CysK, respectively).

Absence of Formation of a CysE-CysK Complex—In Gram-negative bacteria and plants, CysK forms a complex with CysE, called cysteine synthase (10, 31, 34–36). We therefore investigated whether such a complex occurred in *B. subtilis*, because this might influence the association of CysK with CymR. In SPR experiments, no interaction could be detected between MBP-CysK (or CysK, obtained after cleavage of MBP-CysK by factor X) and CysE, with an His tag at either the N or C terminus (data not shown). Similarly, we performed pulldown assays with His₆-CysE and CysK; no CysK was retained on the His₆-CysE column (data not shown). These results indicated that CysE and CysK were not able to form a complex *in vitro* in our experimental conditions. The formation of cysteine synthase has been reported to lead to a decrease of CysK activity in *E. coli* (35) and in plants (37). We however showed that in *B. subtilis*, as expected, CysK activities were similar, whether His₆-CysE was present (240 μ mol of cysteine·min⁻¹·(mg of protein)⁻¹) or absent (255 μ mol of cysteine·min⁻¹·(mg of protein)⁻¹). Moreover, unlike in *E. coli* (10), CysK-His₆ had no impact on His₆-CysE activity in *B. subtilis*; the CysE activities ($1.6 \pm 0.5 \mu$ mol of CoA·min⁻¹·(mg of protein)⁻¹) were similar in the presence or absence of CysK. No interaction between CysE and CysK was detected in yeast two-hybrid assays, in conditions in which both the interaction of CysK with CymR and the dimerization of

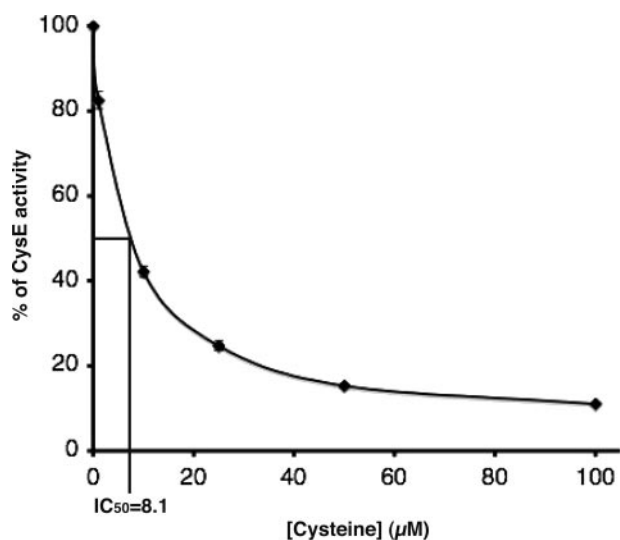


FIGURE 7. Feedback inhibition of CysE by L-cysteine. CysE activity was assayed in the presence of 10 mM serine and increasing L-cysteine concentrations. The activity in the absence of L-cysteine was normalized to 100%.

CysE could be readily detected (Fig. 3). Finally, we also verified by SPR that the addition of CysE had no effect on the CymR-CysK complex formation.

Intracellular Concentrations of CymR, CysK, Cysteine, and OAS in *B. subtilis*—To correlate the data obtained *in vitro* with the physiological situation present in *B. subtilis*, we performed Western blot analyses to estimate the intracellular concentration of CymR and CysK. We used crude extracts of the wild-type strain grown in minimal medium supplemented either with cystine or with methionine. In both cases, we determined a CymR concentration of $0.4 \pm 0.3 \mu\text{M}$, whereas we measured CysK intracellular concentrations of 13 ± 1 and $0.8 \pm 0.3 \mu\text{M}$ in cells grown in the presence of methionine or cystine, respectively. This is in agreement with previous results indicating that the expression of *cysK*, as well as that of other targets of CymR, is high in the presence of methionine and low in the presence of cystine or sulfate (13, 38).

The intracellular concentrations of OAS and cysteine were determined by HPLC in crude extracts of the wild-type strain grown in the presence of either methionine or cystine. The estimated OAS concentration was $184 \pm 43 \mu\text{M}$ in cells grown in the presence of methionine, whereas it was 10-fold lower ($21 \pm 9 \mu\text{M}$) in cells grown in the presence of cystine. In contrast, the intracellular cysteine concentration was $\sim 20 \pm 8 \mu\text{M}$ in the presence of cystine, whereas it was nondetectable in the presence of methionine. This result suggests that, in the presence of cysteine, there is an inhibition of the synthesis and/or the activity of CysE, which catalyzes the production of OAS from serine and acetyl-CoA. It was previously demonstrated that *cysE* expression is regulated by a cysteine-specific T-box (39). We therefore wanted to determine whether cysteine also had a direct impact on CysE activity. As previously demonstrated for other species (8), His₆-CysE activity appeared to be feedback-inhibited by cysteine in *B. subtilis*, because it decreased significantly in the presence of increasing L-cysteine concentrations (Fig. 7). The concentration of cysteine that inhibits 50% of CysE activity (IC_{50}) was estimated at 8.1 ± 1.5

μM (Fig. 7). This *in vitro* value of IC_{50} is in good correlation with the intracellular cysteine concentration ($20 \pm 9 \mu\text{M}$) measured in cells grown in the presence of cystine. The OAS intracellular concentration in the presence of methionine is also in agreement with the $[\text{OAS}]_{50}$ determined in SPR experiments (see above).

DISCUSSION

We here report that CysK, a key enzyme of cysteine synthesis, is a new type of PLP-dependent enzyme playing a regulatory role. Proteins belonging to the ancient, very large, and widely distributed family of PLP-dependent enzymes are mostly involved in various fundamental metabolic pathways. Very few examples of direct involvement of PLP-dependent enzymes in regulatory functions have been described previously. For instance, the GabR regulator of *B. subtilis* contains both a HTH DNA-binding motif and a domain with GABA and aminotransferase activity required for regulation (40). Another example is that of MalY from *E. coli*, which is a cystathione β -lyase acting as a repressor of the maltose regulon by direct interaction with the MalT activator (3, 41). However, the involvement of MalY in the transduction of an unknown signal to MalT remains to be established. Finally, a short isoform of the human branched chain aminotransferase is also a co-repressor for thyroid hormone receptor-mediated transcription by a physical interaction between these two proteins (42).

We demonstrate for the first time that CysK of *B. subtilis* is able to interact physically with the master repressor of cysteine metabolism, CymR (13, 17) and is directly involved in signal transduction to sense the pool of cysteine in the cell. The specific formation of a stable CymR-CysK complex was observed both *in vitro* using pulldown, SPR, and analytical ultracentrifugation and *in vivo* in yeast two-hybrid assays (Figs. 1–3). The affinity of $(\text{CymR})_2$ for $(\text{CysK})_2$ determined by real time SPR ($K_{d1} = 100 \text{ nM}$) is slightly lower than that of the CysK-CysE interaction within the plant or bacterial cysteine synthase ($K_d \approx 3\text{--}40 \text{ nM}$) (10, 37). CymR binds to CysK in a 1:1 molar ratio; a $(\text{CymR})_2$ - $(\text{CysK})_2$ complex is observed at near physiological concentrations, and a $(\text{CymR})_4$ - $(\text{CysK})_4$ complex is observed at higher concentrations. The $(\text{CymR})_2$ - $(\text{CysK})_2$ complex is able to dimerize with a $K_d \sim 10$ -fold higher than the intracellular concentration of CymR ($0.4 \mu\text{M}$).

Each partner in the CymR-CysK complex appears to play a specific role. Contrary to CysK, CymR has a typical HTH motif and is the DNA-binding partner (Fig. 6). Accordingly, we showed that CymR alone is able to bind to the *ytII* promoter region. However, CysK stabilized the CymR-DNA interaction, increasing 7-fold the half-life of this complex in SPR experiments and reducing 20-fold the amount of CymR necessary to observe full retardation in gel shift assays. Per *ytII* promoter region, the interaction involves four CymR molecules, alone or complexed with CysK. Surprisingly, the binding sequence recognized by CymR is neither a direct repeat nor an inverted repeat (13, 20). The mechanism of interaction of CymR with DNA may differ from that of most prokaryotic regulators with a HTH-DNA-binding motif (43). The agreement between the *in vivo* (18, 19) and the *in vitro* data strongly supports the conclusion that CysK directly regulates the CymR-DNA binding activ-

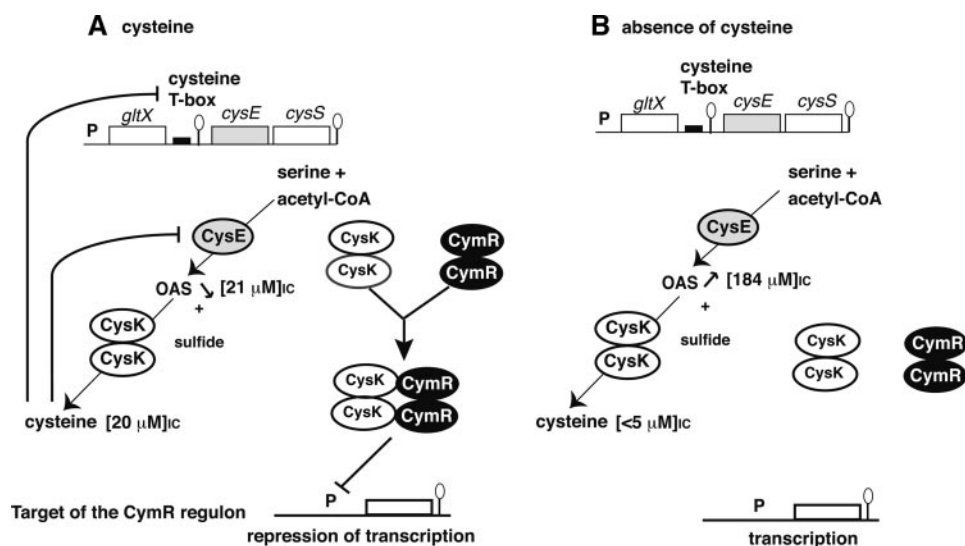


FIGURE 8. Model of the regulation of the cysteine biosynthesis. The model is described in detail under "Discussion." The reactions involved in metabolic pathways are indicated by thin arrows. *cysE*, *cysS*, and *gltX*, encode serine acetyltransferase and cysteinyl and glutamyl tRNA synthetases, respectively. The promoters and terminators are indicated. The motifs involved in premature termination of transcription are indicated by black boxes. The intracellular concentrations of metabolites determined by HPLC are indicated in brackets. OAS, O-acetylserine; acetyl-CoA, acetyl-coenzyme A.

ity via the formation of the CymR-CysK complex. Usually, trigger enzymes negatively modulate the activity of transcription regulators by chelating them under particular growth conditions (2, 6). On the contrary, CysK positively regulates the control of gene expression by CymR. Very recently, another example of positive control by an enzyme has been reported; the glutamine synthetase indeed acts as a chaperone for the GlnR repressor, which controls gene expression in excess nitrogen growth conditions, forming a transient protein-protein interaction stabilizing the GlnR-DNA complexes (44). However, unlike the GlnR-glutamine synthetase system, the CymR-CysK system involves stable regulator-enzyme interactions, allowing us to identify both the binary CymR-CysK complex and the ternary complex with DNA (Figs. 1–3 and 6). To this day, the mechanism of control of CymR by CysK is therefore unique.

We further showed that CysK plays a central role in the response of *B. subtilis* to environmental changes, by signaling cysteine availability to the CymR repressor via the sensing of the concentration of its substrate, OAS. Physiological data and gel shift assays indeed suggest that OAS, the direct precursor of cysteine, is the effector modulating CymR-dependent regulation (13, 19). The serine-transacetylase CysE produces OAS from serine and acetyl-coA. In *B. subtilis*, *cysE* expression is regulated by transcription antitermination at a cysteine-specific T-box (39). We demonstrated that CysE activity is feedback-inhibited by cysteine with an IC_{50} of $8.4 \mu\text{M}$, in the same order as that observed in *E. coli* and plants (Fig. 7) (10, 35). Accordingly, OAS concentration is inversely correlated with that of cysteine *in vivo*. Moreover, SPR experiments indicated that OAS prevents the interaction of CymR with CysK and accelerates the dissociation of preformed CymR/CysK (Fig. 5). A similar role of OAS in the dissociation of the henzym CysE-CysK complex has been demonstrated in *E. coli* and plants (10). Interestingly, the active site of CysK is involved in the interaction with CysE (45, 46). As in the case of the CysE-CysK com-

plex, OAS might induce the dissociation of the CymR-CysK complex either by directly competing with CymR for binding to the active site of CysK or by altering the conformation of CysK indirectly preventing its interaction with CymR. PLP has been reported to stabilize the native fold of most of PLP enzymes (47). In the case of MalY, PLP is also required to maintain it in a conformation capable of interacting with its associated regulator MalT (41, 48). The site of attachment of PLP in CysK, which is involved in OAS binding during catalysis, could also play an essential role for the interaction between CymR and CysK.

Several elements in this elaborate regulation system involving CymR and CysK are interesting from an evolutionary point of view. Members of the Rrf2 family are sensitive

to various metabolites in cell (iron, nitric oxide, and iron-sulfur clusters) via the presence of three conserved cysteine residues, which likely correspond to a iron-sulfur cluster binding site in IscR, NsrR and RirA (14, 49). These cysteine residues are absent in CymR and in a recently identified Rrf2-type regulator, BadM, involved in the control of anaerobic benzoate degradation in *Rhodospseudomonas palustris* (50). CymR-like regulators lacking the cysteine cluster are only found in Bacilli, Staphylococci, Listeria, and some Clostridia. In *Clostridium acetobutylicum*, *Clostridium tetani*, and *Clostridium botulinum*, *cysK* and *cymR*-like genes are adjacent on the chromosome. We propose that CysK has been recruited by CymR to participate in signal transduction of cysteine availability. The complex regulatory mechanism of cysteine metabolism deciphered in *B. subtilis* could be conserved in Bacillales and some Clostridia.

Interestingly, we failed to demonstrate the formation of a henzym cysteine synthase complex between CysK and CysE in *B. subtilis* using a variety of approaches that have been used to demonstrate this interaction in other bacteria and plants: pulldown, yeast two-hybrid, SPR, and enzymatic assays (11, 31, 46, 51, 52). Furthermore, the addition of purified CysK to CysE had no effect on the CysE activity, contrary to what is observed in *E. coli* (10). The only organism in which the absence of interaction between CysK and CysE has been previously demonstrated is the protist parasite Entamoeba, in which the C-terminal helix of CysK occupies the groove that is involved in CysE binding in other organisms (53). This could also be the case for CysK of *B. subtilis*. Another explanation might be the absence of an Ile at the C terminus of CysE of *B. subtilis*, an amino acid that is essential for its interaction with CysK in many organisms (36, 45). Whichever is the case, we propose that in *B. subtilis*, CysK may have lost the capacity to form a cysteine synthase complex with CysE and gained the ability to bind to CymR.

In conclusion, we propose the following model for the regulation of cysteine biosynthesis in *B. subtilis* taking into account the

physiological concentrations of the different proteins and metabolites and the quantitative *in vitro* parameters of the interactions between the different partners (Fig. 8). Changes of OAS concentrations in a narrow range *in vivo* significantly modulate the formation of the CymR-CysK complex. When cysteine is present, the pool of OAS is low and the intracellular concentrations of CymR and CysK are of the same order of magnitude. Under these conditions the CymR-CysK complex is formed, and transcriptional repression of the CymR regulon occurs. In the absence of cysteine, the OAS pool is high. The CymR-CysK complex is mostly dissociated, leading to a faster dissociation of CymR from its DNA targets and the lifting of CymR-dependent repression. This model is an important step in understanding how *B. subtilis* efficiently adapts to environmental changes by linking gene expression to the intracellular pool of a small number of key metabolites as proposed for other regulatory networks (54, 55).

Acknowledgments—We are grateful to E. Courtois, E. Brito, and S. Hoos for technical assistance during this work and to P. Courtin for help with the HPLC analysis. We thank V. Fromion and A. Goelzer for helpful advice on the cysteine metabolism model and stimulating collaboration.

REFERENCES

- Balaji, S., Babu, M. M., and Aravind, L. (2007) *J. Mol. Biol.* **372**, 1108–1122
- Commichau, F. M., and Stulke, J. (2008) *Mol. Microbiol.* **67**, 692–702
- Schreiber, V., Steegborn, C., Clausen, T., Boos, W., and Richet, E. (2000) *Mol. Microbiol.* **35**, 765–776
- Joly, N., Bohm, A., Boos, W., and Richet, E. (2004) *J. Biol. Chem.* **279**, 33123–33130
- Commichau, F. M., Herzberg, C., Tripal, P., Valerius, O., and Stulke, J. (2007) *Mol. Microbiol.* **65**, 642–654
- Wray, L. V., Jr., and Fisher, S. H. (2005) *J. Biol. Chem.* **280**, 33298–33304
- Mehta, P. K., and Christen, P. (2000) *Adv. Enzymol.* **74**, 129–184
- Kredich, N. M. (1996) Biosynthesis of Cysteine. in *Escherichia coli and Salmonella: Cellular and Molecular Biology* (Neidhardt, F. C. ed) pp. 514–527, 2nd Ed., ASM Press, Washington, DC
- Schnell, R., Oehlmann, W., Singh, M., and Schneider, G. (2007) *J. Biol. Chem.* **282**, 23473–23481
- Zhao, C., Moriga, Y., Feng, B., Kumada, Y., Imanaka, H., Imamura, K., and Nakanishi, K. (2006) *Biochem. Biophys. Res. Commun.* **341**, 911–916
- Berkowitz, O., Wirtz, M., Wolf, A., Kuhlmann, J., and Hell, R. (2002) *J. Biol. Chem.* **277**, 30629–30634
- Guédon, E., and Martin-Verstraete, I. (2007) in *Amino Acid Biosynthesis: Pathways, Regulation and Metabolic Engineering*. (Wendisch, V. F., ed) pp. 195–218, Springer, Berlin Heidelberg, Germany
- Even, S., Burguière, P., Auger, S., Soutourina, O., Danchin, A., and Martin-Verstraete, I. (2006) *J. Bacteriol.* **188**, 2184–2197
- Schwartz, C. J., Giel, J. L., Patschkowski, T., Luther, C., Ruzicka, F. J., Beinert, H., and Kiley, P. J. (2001) *Proc. Natl. Acad. Sci. U. S. A.* **98**, 14895–14900
- Giel, J. L., Rodionov, D., Liu, M., Blattner, F. R., and Kiley, P. J. (2006) *Mol. Microbiol.* **60**, 1058–1075
- Viguier, C., P. O. C., Clarke, P., and O'Connell, M. (2005) *FEMS Microbiol. Lett.* **246**, 235–242
- Choi, S. Y., Reyes, D., Leelakriangsak, M., and Zuber, P. (2006) *J. Bacteriol.* **188**, 5741–5751
- Albanesi, D., Mansilla, M. C., Schujman, G. E., and de Mendoza, D. (2005) *J. Bacteriol.* **187**, 7631–7638
- Hullo, M. F., Auger, S., Soutourina, O., Barzu, O., Yvon, M., Danchin, A., and Martin-Verstraete, I. (2007) *J. Bacteriol.* **189**, 187–197
- Burguière, P., Fert, J., Guillaouard, I., Auger, S., Danchin, A., and Martin-Verstraete, I. (2005) *J. Bacteriol.* **187**, 6019–6030
- van der Ploeg, J. R., Barone, M., and Leisinger, T. (2001) *FEMS Microbiol. Lett.* **201**, 29–35
- James, P., Halladay, J., and Craig, E. A. (1996) *Genetics* **144**, 1425–1436
- Noirot-Gros, M. F., Velten, M., Yoshimura, M., McGovern, S., Morimoto, T., Ehrlich, S. D., Ogasawara, N., Polard, P., and Noirot, P. (2006) *Proc. Natl. Acad. Sci. U. S. A.* **103**, 2368–2373
- Veiga, P., Bulbarello-Sampieri, C., Furlan, S., Maisons, A., Chapot-Chartier, M. P., Erkelenz, M., Mervelet, P., Noirot, P., Frees, D., Kuipers, O. P., Kok, J., Gruss, A., Buist, G., and Kulakauskas, S. (2007) *J. Biol. Chem.* **282**, 19342–19354
- Munier, H., Gilles, A. M., Glaser, P., Krin, E., Danchin, A., Sarfati, R., and Barzu, O. (1991) *Eur. J. Biochem.* **196**, 469–474
- England, P., Bregerege, F., and Bedouelle, H. (1997) *Biochemistry* **36**, 164–172
- Schuck, P. (2000) *Biophys. J.* **78**, 1606–1619
- Demeler, B. (2005) in *Modern Analytical Ultracentrifugation: Techniques and Methods* (Scott, D. J., Harding, S. E., and Rowe, A. J., eds) pp. 210–230, Royal Society of Chemistry, Cambridge, United Kingdom
- Denk, D., and Bock, A. (1987) *J. Gen. Microbiol.* **133**, 515–525
- Holtmann, G., and Bremer, E. (2004) *J. Bacteriol.* **186**, 1683–1693
- Bogdanova, N., and Hell, R. (1997) *Plant J.* **11**, 251–262
- Liszewska, F., Lewandowska, M., Plochocka, D., and Sirko, A. (2007) *Biochim. Biophys. Acta* **1774**, 450–455
- Byrne, C. R., Monroe, R. S., Ward, K. A., and Kredich, N. M. (1988) *J. Bacteriol.* **170**, 3150–3157
- Kredich, N. M., Becker, M. A., and Tomkins, G. M. (1969) *J. Biol. Chem.* **244**, 2428–2439
- Mino, K., Imamura, K., Sakiyama, T., Eisaki, N., Matsuyama, A., and Nakanishi, K. (2001) *Biosci. Biotechnol. Biochem.* **65**, 865–874
- Huang, B., Vetting, M. W., and Roderick, S. L. (2005) *J. Bacteriol.* **187**, 3201–3205
- Droux, M., Ruffet, M. L., Douce, R., and Job, D. (1998) *Eur. J. Biochem.* **255**, 235–245
- Auger, S., Danchin, A., and Martin-Verstraete, I. (2002) *J. Bacteriol.* **184**, 5179–5186
- Gagnon, Y., Breton, R., Putzer, H., Pelchat, M., Grunberg-Manago, M., and Lapointe, J. (1994) *J. Biol. Chem.* **269**, 7473–7482
- Belitsky, B. R. (2004) *J. Mol. Biol.* **340**, 655–664
- Clausen, T., Schlegel, A., Peist, R., Schneider, E., Steegborn, C., Chang, Y. S., Haase, A., Bourenkov, G. P., Bartunik, H. D., and Boos, W. (2000) *EMBO J.* **19**, 831–842
- Lin, H. M., Kaneshige, M., Zhao, L., Zhang, X., Hanover, J. A., and Cheng, S. Y. (2001) *J. Biol. Chem.* **276**, 48196–48205
- Huffman, J. L., and Brennan, R. G. (2002) *Curr. Opin. Struct. Biol.* **12**, 98–106
- Fisher, S. H., and Wray, L. V., Jr. (2008) *Proc. Natl. Acad. Sci. U. S. A.* **105**, 1014–1019
- Francois, J. A., Kumaran, S., and Jez, J. M. (2006) *Plant Cell* **18**, 3647–3655
- Bonner, E. R., Cahoon, R. E., Knapke, S. M., and Jez, J. M. (2005) *J. Biol. Chem.* **280**, 38803–38813
- Bettati, S., Benci, S., Campanini, B., Raboni, S., Chirico, G., Beretta, S., Schnackerz, K. D., Hazlett, T. L., Gratton, E., and Mozzarelli, A. (2000) *J. Biol. Chem.* **275**, 40244–40251
- Bertoldi, M., Cellini, B., Laurents, D. V., and Voltattorni, C. B. (2005) *Biochemical J.* **389**, 885–898
- Bodenmiller, D. M., and Spiro, S. (2006) *J. Bacteriol.* **188**, 874–881
- Peres, C. M., and Harwood, C. S. (2006) *J. Bacteriol.* **188**, 8662–8665
- Mino, K., Yamanoue, T., Sakiyama, T., Eisaki, N., Matsuyama, A., and Nakanishi, K. (1999) *Biosci. Biotechnol. Biochem.* **63**, 168–179
- Wirtz, M., Berkowitz, O., Droux, M., and Hell, R. (2001) *Eur. J. Biochem.* **268**, 686–693
- Chinthalapudi, K., Kumar, M., Kumar, S., Jain, S., Alam, N., and Gourinath, S. (2008) *Proteins* **72**, 1222–1232
- Sonenshein, A. L. (2007) *Nat. Rev. Microbiol.* **5**, 917–927
- Goelzer, A., Bekkal Brikci, F., Martin-Verstraete, I., Noirot, P., Bessieres, P., Aymerich, S., and Fromion, V. (2008) *BMC Syst. Biol.* **2**, 20
- Auger, S., Gomez, M. P., Danchin, A., and Martin-Verstraete, I. (2005) *Biochimie (Paris)* **87**, 231–238